OG 981

BNL--40536

DE88 004858

JAN 2 5 1988

MEASUREMENT OF ENERGY AND CHARGED PARTICLE EMISSION IN THE CENTRAL RAPIDITY REGION FROM O+A AND p+A COLLISIONS AT 14.5 GeV/c PER NUCLEON AND PRELIMINARY RESULTS FROM Si+A COLLISIONS#

E-802 Collaboration, Brookhaven National Laboratory, Upton, NY 11973
ANL-BNL-Columbia-Hiroshima-LBL-MIT-UCBerkeley-UCRiverside-Tokyo

T. ABBOTT[g], Y. AKIBA[i,*], D. ALBURGER[b], D. BEAVIS[b], R.R. BETTS[a], M.A. BLOOMER[f], P.D. BOND[b], C. CHASMAN[b], Y.Y. CHU[b], B.A. COLE[f], J.B. COSTALES[f], H. CRAWFORD[h], J.B. CUMMING[b], R. DEBBE[b], E. DUEK[b], H.A. ENGE[f], J. ENGELAGE[h], S.Y. FUNG[g], D. GREINER[e], L. GRODZINS[f], S. GUSHUE[b], H. HAMAGAKI[j], O. HANSEN[b], P. HAUSTEIN[b], S. HAYASHI[j], S. HOMMA[j], H.Z. HUANG[f], Y. IKEDA[j], S. KATCOFF[b], S. KAUFMAN[a], R.J. LEDOUX[f], M.J. LE VINE[b], P. LINDSTROM[e], M.A.J. MARISCOTTI[b,**], Y. MIAKE[b,***], R. MORSE[f], S. NAGAMIYA[c,***], J. OLNESS[b], C. PARSONS[f], L.P. REMSBERG[b], M. SARABURA[f], A. SHOR[b], S.G. STEADMAN[f], G.S.F. STEPHANS[f], T. SUGITATE[d], A.W. SUNYAR[b,+], M. TANAKA[b], M.J. TANNENBAUM[b], M. TORIKOSHI[b], J.H. VAN DIJK[b], F. VIDEBAEK[a], P. VINCENT[b], E. VULGARIS[f], V. VUTSADAKIS[f], W.A. WATSON III[b], H.E. WEGNER[b], D.S. WOODRUFF[f], and W. ZAJC[c]

a Argonne National Laboratory, Argonne, IL 60439
b Brookhaven National Laboratory, Upton, NY 11973
c Columbia University, New York, NY 10027 and Nevis Laboratories, Irvington, NY 10533
d Hiroshima University, Hiroshima 730, JAPAN
e Lawrence Berkeley Laboratory, Berkeley, CA 94720
f Massachusetts Institute of Technology, Cambridge, MA 02139
g University of California, Riverside, CA 92507
h Univ. of California, Space Sciences Laboratory, Berkeley, CA 94720
i University of Tokyo, Department of Physics, Tokyo 113, JAPAN
j University of Tokyo, Institute for Nuclear Study, Tokyo 188, JAPAN

Presented by L.P.Remsberg and M.J.Tannenbaum

* JSPS Fellowship for Japanese Junior Scientists
** On leave of absence from Comision Nacional de Energia Atomica, Buenos Aires, ARGENTINA
*** On leave of absence from University of Tokyo
+ Deceased

To appear in Quark-Matter 1987 Proceedings.

MASTER

DISTRIBUTION OF THIS DOCUMENT IS UNLIMITED

ABSTRACT

The first data from a 16O beam of total energy 232 GeV at the BNL Tandem-AGS are discussed. Preliminary results from a 28Si beam of total energy 406 GeV are also shown. The full complement of E-802, including a magnetic spectrometer, was used for the 28Si measurement. A different experimental arrangement was used for 16O. Comparison measurements with proton beams are presented for both configurations.

I INTRODUCTION

In the spring of 1987, E-802 in its full configuration [1] took data with a silicon beam. In addition, during the machine development run in the fall of 1986, a smaller experiment was assembled from components of E802, and measurements were made using an oxygen beam of momentum 14.5 GeV/c per nucleon. The smaller experiment consisted of a series of scintillation counters to define the beam geometry and purity, a full azimuth lead glass array, and the wall of the target multiplicity array (TMA). Some results from these measurements have already been published [2].

II EXPERIMENTAL ARRANGEMENT FOR OXYGEN RUNS

A 16O beam of total energy 232 GeV was extracted from the Tandem-AGS and focussed to a beam spot of ~2mm x 2mm at the target. To minimize the effects of pile-up and secondary projectile interactions, the beam intensity was collimated down to 10,000 ions per pulse (400 ms spill), and the thickness of the various targets was kept roughly the same in interaction probability (~2%). The purity of the beam (Z=8) was measured to be >99%. Located 65 cm downstream of the target, the TMA wall of proportional counter tubes with 1536 readout pads was used to measure the charged particle multiplicity. The TMA wall was rectangular with dimension 90 cm. wide by 53 cm. high. A square array of 96 lead glass blocks (PbGl) was placed 1 meter downstream of the target. This array was 10 blocks wide by 10 high with a 2 by 2 block hole in the center for the beam to pass through. The PbGl array measured the electromagnetic energy emitted in a laboratory polar angular interval from 10 to 32 degrees. In the nucleon-nucleon center of mass reference frame, this corresponded to a pseudo-rapidity coverage of ~ $-0.5<\eta<0.7$. The corresponding range for the TMA was ~ $-0.6<\eta<1.1$. In this experimental arrangement, both detectors had full azimuthal coverage.

Triggers were provided by a bullseye counter or by an analog sum of the outputs of the 96 PbGl photomultipliers, corresponding to the total energy recorded with no transverse weighting. The pulse height spectrum observed in the bullseye counter is shown in figure 1. The oxygen peak was obtained from a sample of non-interacting beam particles, and has been superimposed onto the data from the PbGl triggers. When energy is observed in the PbGl, the oxygen peak vanishes and is replaced by structures

corresponding to nitrogen, carbon and boron, followed by a continuum distribution at lower pulse heights.

III RESULTS FROM 16O+A AND p+A COLLISIONS

The spectrum of energy observed in the PbGl is shown in figure 2 for oxygen interactions on Au, Cu, and mylar targets and for positive hadron (80% proton) [2] interactions on an Au target , all measured at 14.5 GeV/c per nucleon in the same experimental arrangement. The observed energy is denoted E(0,TOT) since the PbGl responds primarily to neutral mesons, pizero and eta-zero, which are detected via their two-photon decay. Relativistic charged hadrons (v/c > 0.8) also emit Cerenkov light in the PbGl, equivalent to approximately 500 MeV per particle, and contribute, in this particular configuration, on the average, about 50% of the observed energy. The response of the PbGl to Cerenkov light is linear to <1%, whatever the source. The gains of all the individual blocks were monitored with 241Am-CsI light pulsers [3], so that the relative scale variation of E(0,TOT) is better than +/- 1% for the 16O data and +/- 5% for the proton data. The absolute scale of E(0,TOT) was set by calibration in an electron beam. No attempt was made to correct E(0,TOT) on an event by event basis for the Cerenkov light from charged hadrons. The two lower scales on figure 2 were estimated using an average correction (see discussion below).

The E(0,TOT) spectrum for 16O+Au shows a broad plateau, a peak centered at 40 GeV and then a sharp drop-off until the yield runs out at ~ 70 GeV (see fig. 2). The 16O+Cu data also show evidence of considerable energy emission, even though the maximum thickness of a Cu nucleus is only ~2/3 that of Au. It is of particular interest that the edges of the 16O+Cu and 16O+Au spectra become virtually identical above 50 GeV if the Cu cross section is multiplied by a factor of ~6.

The charged-particle multiplicity spectra for oxygen interactions with C, Cu and Au as well as protons with Au are shown in figure 3. The TMA is sensitive to all charged particles with a range greater than that of ~ 30 MeV protons. The general appearance of the charged-particle spectra is similar to that of the E(0,TOT) spectra. However, it is clear that the high-multiplicity edge of the 16O+Au distribution extends well beyond that of 16O+Cu, in contrast to the behavior of the E(0,TOT) spectra.

The correlation between the charged-particle multiplicity and E(0,TOT) for 16O+Au is shown in figure 4. For these data, the acceptance of the TMA wall was restricted so that only particles which could pass through the PbGl were included. The TMA coverage for figure 4 corresponds to ~ 80% of the number of particles incident on the PbGl. The multiplicity and E(0,TOT) show a strong linear correlation demonstrating that the value of E(0,TOT) is proportional to the number of charged particles.

IV ANALYSIS OF PBGL DATA IN p+A, 16O+Au and 16O+Cu COLLISIONS

The features of the E(O,TOT) spectra can be described by a simple, geometrical model, based on the observation at 200 GeV/u [4] that the high energy edge of the 16O+Au spectrum is just the 16-fold convolution of the p+Au spectrum. The convolution is easily performed by using a gamma distribution [5] to fit the p+Au E(O,TOT) spectrum as shown in fig. 5 (broken line). The form of the distribution is:

$$f(E) = (b/GAM(p))*((bE)**(p-1))*exp(-bE). \qquad (1)$$

where E is the observed energy (E(O,TOT)), b and p are parameters, and GAM(p) denotes the gamma function. For the present p+Au data the best fit parameters are b = 0.95+/- 0.09 GeV**(-1), p = 2.60+/- 0.24, with average energy ‹E(O,TOT)› = p/b = 2.73 GeV. The n-th convolution of this distribution is obtained by holding the parameter b constant and letting p --› np. The high energy edge of the O+Au spectrum, E(O,TOT) › 45 GeV, can also be fit to a single gamma distribution (1). With the parameter b held constant at 0.95, the best fit (fig 6, broken curve) corresponds to 26% of the observed O+Au cross section and 16 convolutions of the observed p+Au spectrum, in excellent agreement with the original NA35 observation [4]. However, the situation is more complicated than this simple procedure, as will be discussed below.

Note that the charged multiplicity distributions do not obey this simple convolution analysis. The average p+Au multiplicity multiplied by 16 equals 91, which is well out on the tail of the 16O+Au distribution and well beyond the maximum multiplicity recorded for 16O+Cu (see figure 3). At least part of the explanation of this result may stem from the substantial difference in the response of the TMA and PbGl detectors to soft target protons.

The model for the high-energy edge of the PbGl data can be extended to describe the entire E(O,TOT) spectra for 16O+Cu and 16O+Au collisions. The observed p+Au spectrum is convoluted from 1 to 16 times, with weights for the n-fold convolutions obtained from a Monte Carlo calculation [6] which averages over the impact parameter of the nucleus-nucleus collision to obtain the distribution in the number of projectile nucleons which interact at least once in the target. Woods-Saxon densities are assumed for both the beam and target nuclei and a p-p inelastic cross section of 30 mb is used corresponding to a nucleon-nucleon mean free path of ~2.2 fm. Two sets of parameters have been used for the nuclear densities. In our recent publication [2], the density function used was:

$$F(r)=1.0/(1.0+exp((r-c)/a0)) \qquad (2)$$

with c = 1.14 x A**1/3 fm and a0 = 0.05 fm. The value for the radius is reasonable, but the diffusivity, a0, gives a distribution nearly identical to a sharp sphere and is therefore too small. In this work, more realistic parameters are used [7]. For Cu and Au, equation (2) is used, with

$$c=1.18 \times A^{**1/3} - 0.48 \text{ fm} \quad \text{and } a0 = 0.545 \text{ fm}.$$

The density function for oxygen is

$$G(r) = F(r) \times (1.0 - 0.051 \times r^{**2}/c^{**2})$$

with F(r) given by equation (2) with c=2.608 fm and a0 = 0.513 fm. Excellent representations of both the 16O+Au and 16O+Cu spectra are obtained from this "wounded-projectile-nucleon" (WPN) model (see fig. 7) [8]. It then appears that the peak in the 16O+Au spectrum and the identical shape of the high-energy edges of the 16O+Au and 16O+Cu spectra arise from events in which all 16 projectile nucleons interact.

Although the naive WPN model seems quite reasonable and fits the data rather well, it is in serious contradiction with the understanding of relativistic nuclear interactions gleaned from proton-nucleus collisions [9]. When a proton passes through a nucleus, it can make several successive interactions. However, the observed multiplicity in p+A collisions is not simply proportional to the number of interactions but increases much more slowly. For instance, in a p+Au collision there are on the average 4.2 nucleon-nucleon interactions but the observed maximum multiplicity density increases only by a factor of ~2 [10]. Most of the effort in theories of the collisions of protons with nuclei has gone into trying to understand how the effects of the successive interactions are suppressed. One of these models is the Wounded-Nucleon Model (WNM) [11], in which a nucleon contributes only once to the production of particles no matter how many times (>_ 1) it is successively struck.

To illustrate this point, a proper Wounded-Nucleon Model (WNM) calculation was done. The distributions in the number of wounded nucleons were obtained from the above Monte Carlo, but this time the WNM algorithm [11] was applied. The solid line in figure 5 is the WNM fit to the p+Au spectrum composed of the weighted sum of 2,3,4,,,14 wounded nucleons (dotted lines). The weights are from the nearly sharp sphere potential. The parameters fitted in this deconvolution represent the shape of the proton-proton E(0,TOT) spectrum, assumed to obey equation (1), b(p-p) = 2.90+/- 0.78 GeV**(-1), p(p-p) = 2.99+/- 0.84, with average energy <E(0,TOT)>(p-p) = 1.03 GeV. These parameters with the appropriate WNM weights are then used to reconstruct the WNM predictions for 16O+Au and 16O+Cu (figure 8, broken lines). The failure of the WNM to represent the data is particularly striking in comparison to the WPN calculations (figure 8, solid and dotted lines).

It is not difficult to understand a reason for the failure of the WNM in nucleus-nucleus collisions. The WNM algorithm [11] of suppressing the effect of a projectile nucleon making successive interactions in the target also has the consequence of suppressing the effect of target nucleons making successive interactions with the projectile. This is especially significant for the case of central collisions, leading to a prediction of much lower energy emission than is actually observed. The more naive WPN, discussed above, overcomes this problem, but does it by treating the projectile and target nucleons inconsistently: the effect of successive interactions of projectile nucleons in the target is suppressed (by utilization of the observed p+Au spectrum), whereas the effect of target nucleons which are successively struck by multiple projectile nucleons is not suppressed, but the energy emitted is taken as linear in the number of interactions, as apparently indicated by the measurements. Another, related, inconsistency in the WPN is that the observed p+Au spectrum, which is necessarily averaged over all impact parameters, was used for the 16-fold convolution, whereas, it would seem that a "centrally averaged" p+Au or p+Cu spectrum would be more appropriate.

A simple resolution of both these inconsistencies is to presume that the incoming nucleon loses most of its energy in the first few interactions. The subsequent lower energy interactions would be unlikely to produce energy observable in the PbGl (neutral-mesons). In this way the energy emitted in the p+Au system would not depend much on impact parameter, and it is appropriate to use the experimental p+Au spectrum to analyze the 16O+Cu and 16O+Au data. The maximum energy observed in these reactions occurs when all sixteen projectile nucleons interact: i.e., for collisions in which the impact parameter is sufficiently small to allow complete overlap of the 16O+Au or 16O+Cu nuclei. The cross sections for maximum energy deposit in Au and Cu are then in the ratio of these impact parameters squared, ([R(Au)-R(16O)]/[R(Cu)-R(16O)])**2 , a factor of ~5, which is close to the factor of ~ 6 observed.

An estimate of the total transverse energy emitted for central collisions can be made from the data in fig. 2. Since the edges of the spectra are identical above E(0,TOT) = 50 GeV, this value is taken to represent the energy observed in the PbGl for central 16O+Cu or 16O+Au collisions. In order to find the true energy from neutral-meson emission a correction must be made for the fraction of the signal arising from charged hadrons. This fraction is estimated [2] to be 0.5, which results in a neutral energy emission of 25 GeV. The standard assumption is that the total energy is 3 times the neutral, which implies a total energy emission of 75 GeV into the pseudo-rapidity interval -0.5<eta<0.7. If the transverse energy density in pseudo-rapidity is constant in this interval, the appropriate <sin(TH)> is 0.29, which gives a transverse energy of 22 GeV or dE(T)/d(eta) = 18 GeV. The Bjorken formula [12], although it may not be appropriate in this domain, then gives an energy density of 0.7 GeV/fm**3 for a formation time of 1 fm. A

similar value is obtained from a fireball model calculation for 16O+Cu. This result is about 40% of the NA35 published value at 200 GeV/per nucleon in a comparable pseudo rapidity interval[4]. The two lower scales on figure 2 correspond to the total energy, E(TOT), and transverse energy, E(T), as derived with the average corrections just discussed.

V CONCLUSIONS FROM 16O+A and p+A MEASUREMENTS

The observation that the maximum energy emitted in 16O+Cu collisions is essentially the same as in 16O+Au collisions (see Fig. 2) shows that the 16O projectiles can be sufficiently stopped in Cu so that pion emission effectively ceases. The cross sections near the maximum observed E(0,TOT) can be understood by simple geometrical arguments if it is assumed that only a few nucleon-nucleon interactions are required to exhaust the energy of the incoming nucleon. Surprisingly, the p+Au E(0,TOT) spectrum can be used to reconstruct the entire 16O+Au and 16O+Cu spectra, which lends further support to this argument.

VI PRELIMINARY PBGL RESULTS FROM SPRING 1987 RUNS WITH SILICON

Preliminary results are available from the run in spring 1987 with silicon and proton beams at 14.5 GeV/c per nucleon. For this series of measurements, the protons were identified by a Cerenkov counter in the positive hadron beam. The PbGl consisted of 245 blocks located 3 meters downstream of the target and covered approximately the same laboratory polar angular interval as the small experiment, from 10 to 30 degrees, but only covered 1/2 of the azimuth. The magnetic spectrometer occupied the other half of the azimuth. Because of the greater distance from the target, the angular segmentation of the PbGl for this run was three times finer in both polar and azimuthal angles than for the fall 1986 run.

The first data to be presented from this 1/2 azimuth configuration are proton measurements with targets of Au, Cu, Al and C (figure 9). The shapes of the spectra are virtually the same for all the targets, which is consistent with the presumption of the projectile losing most of its energy in the first few interactions. These spectra can be fit to equation (1) and all give the same value of b=1.29 GeV**(-1). It is important to note that acceptance effects may be very significant in these spectra since the detector is too small to be struck with ~100% probability on every p-p inelastic collision.

The improved granularity of the PbGl allows both E(0,TOT) and E(0,T) spectra to be obtained. The data are shown in figure 10 for Si interactions on Au and Al. The energy scale for both E(0,TOT) and E(0,T) is normalized by the average value in each case. Note that the shapes of the spectra are essentially identical in both E(0,TOT) and E(0,T). This is consistent with the fact that the detector covers a limited pseudo-rapidity interval and with the

assumption made above that the transverse energy density in pseudo-rapidity is constant in this interval. The fact that the shapes of the spectra agree so well implies that the granularity of the detector preserves the resolution in going from energy to transverse energy. If one may go out on a limb a bit, careful inspection of figure 10 indicates that the E(0,T) spectrum is slightly lower than the E(0,TOT) spectrum in Si+Al but slightly higher in Si+Au. This implies that the energy emission is at slightly larger angles for the Au target than for Al, and is a gauge of the small size of the effect of rescattering and successive interactions in the two different target nuclei.

A final comment on figure 10 concerns the much broader shape, in units of the mean value, of the Si+Al spectrum compared to the Si+Au spectrum. This is simply a consequence of the fact that the Si+Au spectrum has a flat plateau, and then a sharp drop-off at high energy, while the Si+Al data just drops off continuously, without a plateau. The mean value of the energy for the Si+Au data is near the center of the plateau, and is thus shifted higher relative to the slope of the drop-off than is the case for the Si+Al data. This can be seen more clearly from figure 11 where the E(0,TOT) spectra for the spring 1987 configuration are shown. The spectrum for proton interactions on an Au target is included for comparison with the spectra for silicon interactions on Au and Al targets. These data look very similar to the spectra from the fall 1986 configuration with oxygen (figure 2) but a quantitative comparison is difficult at this time because of the different solid angles for the two experimental arrangements. It is however possible to ask whether the upper edge of the Si+Au spectrum, E(0,TOT) > 40 GeV, is consistent with 28 p+Au interactions. The fit, shown in figure 12, corresponds to 11% of the observed Si+Au cross section and 27 convolutions of the observed p+Au spectrum in this configuration, and is consistent with all the projectile nucleons interacting. Acceptance effects are important in the interpretation of these preliminary spectra, and more targets are needed. The work is continuing.

ACKNOWLEDGEMENT

E-802 experiments are supported in part by the U.S. Department of Energy under contracts with ANL, BNL, Columbia, LBL, MIT, and UC Riverside, in part by the NASA under contract with the University of California and by the US-Japan High Energy Physics Collaboration Treaty. We are particularly indebted to K. Asselta, E. Baker, D. Dayton, H. Diaz, J. Dioguardi, M. Manni, R. Scheetz, and D. Tuttle for their support in all technical aspects of the experiment. We are also pleased to acknowledge the expertise of the AGS and the Tandem Operations staffs in providing the beams.

References

[1] E-802 Collaboration, T.Abbott et. al., accompanying paper in these proceedings.

[2] E-802 Collaboration, T.Abbott et al., Phys. Lett. B197 (1987) 285.

[3] D.E.Alburger et al., Nucl. Instr. and Meth. A254 (1987) 88.

[4] NA35 Collaboration, A.Bamberger et al., Phys. Lett. B184 (1987) 271.

[5] BCMOR Collaboration, A.L.S. Angelis et al., Phys. Lett. 168B (1986) 158; 141B (1984) 140. See also M.J. Tannenbaum et al, Proc. Quark Matter 1984, editor K. Kajantie (Springer, Berlin 1985), pp. 174-186; B. Callen et al., ibid. pp. 133-142.

[6] H.Brody et al., Phys. Rev. D28 (1983) 2334.

[7] M.A.Preston and R.K.Bhaduri, Structure of the Nucleus (Addison Wesley, Reading, Mass. 1975); C.W.Dejager, H.DeVries and C.DeVries, Atomic Data and Nuclear Data Tables, 14 (1974) 479.

[8] A similar analysis for the NA35 data was performed by J.Ftacnik et al., Phys. Lett. B188 (1987) 279.

[9] P.M.Fishbane and J.S.Trefil, Phys. Rev. D9 (1974) 168; Phys. Lett. 51B (1974) 139; K.Gottfried, Phys. Rev. Lett. 32 (1974) 957.

[10] W.Busza et al., Phys. Rev. Lett. 34 (1975) 836; E.Dengler et al., Z. Phys. C33 (1986) 187.

[11] A.Bialas, A.Bleszynski & W.Czyz, Nucl. Phys. B111 (1976) 461.

[12] J.D.Bjorken, Phys. Rev. D27 (1983) 140.

DISCLAIMER

This report was prepared as an account of work sponsored by an agency of the United States Government. Neither the United States Government nor any agency thereof, nor any of their employees, makes any warranty, express or implied, or assumes any legal liability or responsibility for the accuracy, completeness, or usefulness of any information, apparatus, product, or process disclosed, or represents that its use would not infringe privately owned rights. Reference herein to any specific commercial product, process, or service by trade name, trademark, manufacturer, or otherwise does not necessarily constitute or imply its endorsement, recommendation, or favoring by the United States Government or any agency thereof. The views and opinions of authors expressed herein do not necessarily state or reflect those of the United States Government or any agency thereof.

Figure Captions

Fig. 1 : The pulse height spectrum measured in the bullseye counter. The oxygen peak is obtained from a sample of non-interacting beam particles and superimposed onto the data from the PbGl triggers.

Fig. 2 : Differential cross sections in E(O,TOT), the energy recorded in the PbGl, for 16O interactions on Au, Cu, and Mylar ($C_5H_4O_2$) targets and for proton interactions on an Au target. The errors shown are statistical and include the effect of point by point target-out correction. The p+Au cross section has been divided by a factor of 20 for clarity of presentation. The projectile total energy was 14.5 GeV/u. The two lower scales on the figure correspond approximately to the total energy and transverse energy falling on the detector and have been estimated with an average correction as discussed in the text.

Fig. 3. Differential cross sections in the charged-particle multiplicity measured in the TMA wall for 16O interactions on Au, Cu and C targets and for proton interactions on an Au target. The errors shown are statistical and include the effect of point by point target out correction. The p+Au cross section has been divided by a factor of 20 for clarity of presentation. The average multiplicity for each data set is indicated on the figure.

Fig. 4: The correlation between the charged-particle multiplicity and E(O,TOT) for 16O+Au interactions.

Fig. 5 : E(O,TOT) spectrum for p+Au. The broken line is a fit to a single gamma distribution. The solid line is a Wounded Nucleon Model fit, composed of a sum of the derived spectra for 2,3,4,,,14 wounded nucleons (dotted lines).

Fig. 6 : Fit to the high energy edge of the O+Au E(O,TOT) spectrum as the n-th convolution of the measured p+Au spectrum (broken curve). Only data points with E(O,TOT) > 45 GeV are used for the fit.

Fig. 7 : Measured E(O,TOT) spectra for 16O interactions on Au (a) and Cu (b) together with the sum of 1 to 16-fold convolutions of the measured p+Au spectrum weighted according to the probability for 1,2,,,16 of the projectile nucleons to interact in the target. The individual components of the sum are also shown.

Fig. 8 : The measured E(O,TOT) spectra for 16O interactions on Au (a) and Cu (b) together with three predictions. The solid line is the WPN calculation with Woods-Saxon densities given in the text. The dotted line is the sharp sphere WPN calculation [2]. The broken line is the Wounded Nucleon Model calculation.

Fig. 9 : Preliminary results from the spring 1987 run for proton

interactions on Au, Cu, Al and C targets measured in the half-azimuth fine-granularity lead glass array.

Fig. 10 : Preliminary spectra of energy distributions measured in the fine-granularity half-azimuth lead glass array for silicon interactions on Au (a) and Al (b) targets. The energy scales for transverse energy, E(0,T), and total energy, E(0,TOT), have been normalized by the average values for the distribution, in each case, so that the shapes of the distributions may be easily compared.

Fig. 11 : Preliminary results from the spring 1987 run for 28Si interactions on Au and Al targets and proton interactions on an Au target measured in the half-azimuth fine-granularity lead glass array. The p+Au cross section has been divided by a factor of 20 for clarity of presentation.

Fig. 12 : Fit to the high energy edge of the Si+Au E(0,TOT) spectrum as the n-th convolution of the observed p+Au spectrum in this configuration (broken line). Only data points with E(0,TOT) $>$ 40 GeV are used for the fit.

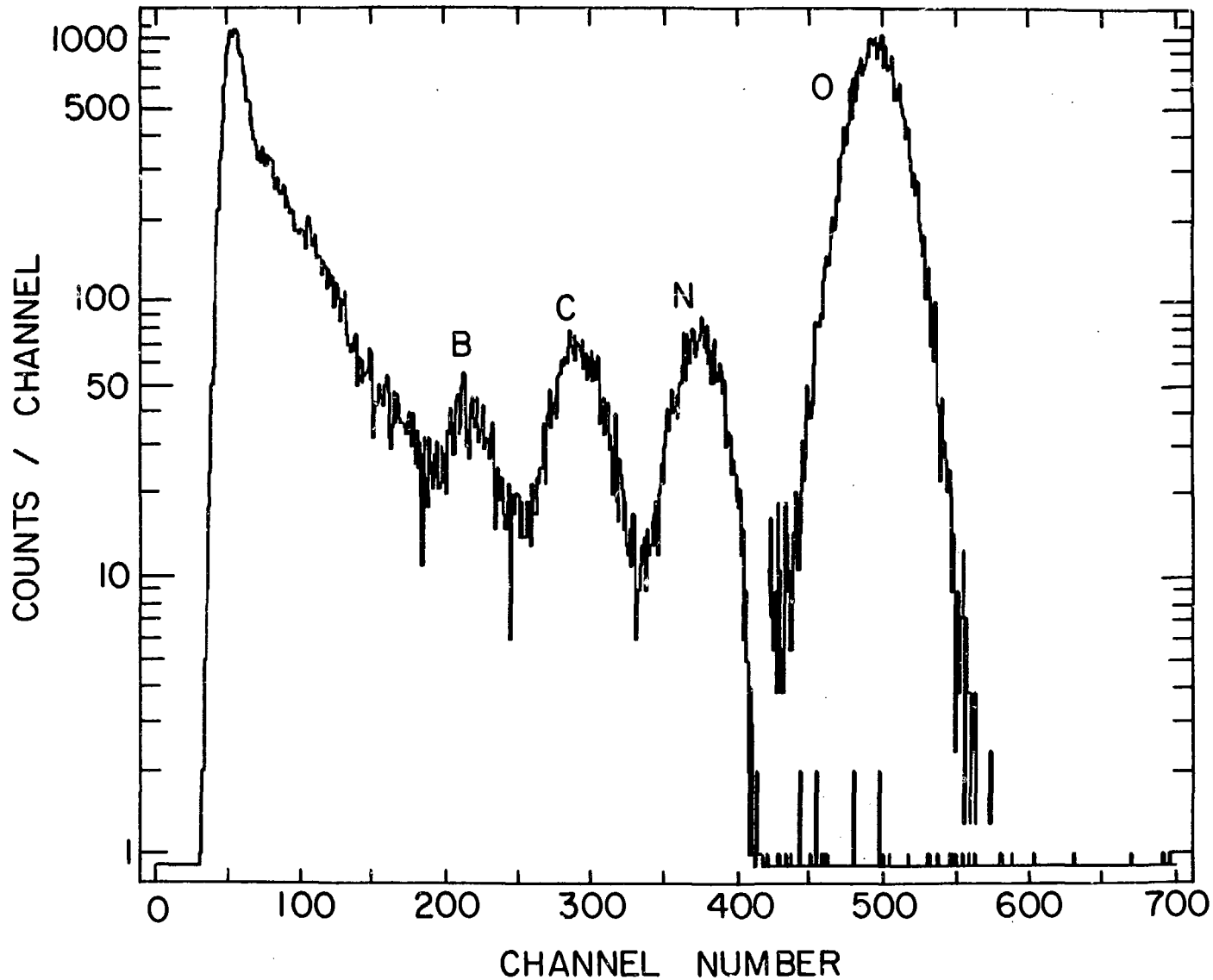
1000
500
100
50
10
1
COUNTS / CHANNEL
B
C
N
O
0
100
200
300
400
500
600
700
CHANNEL NUMBER

Fig. 1

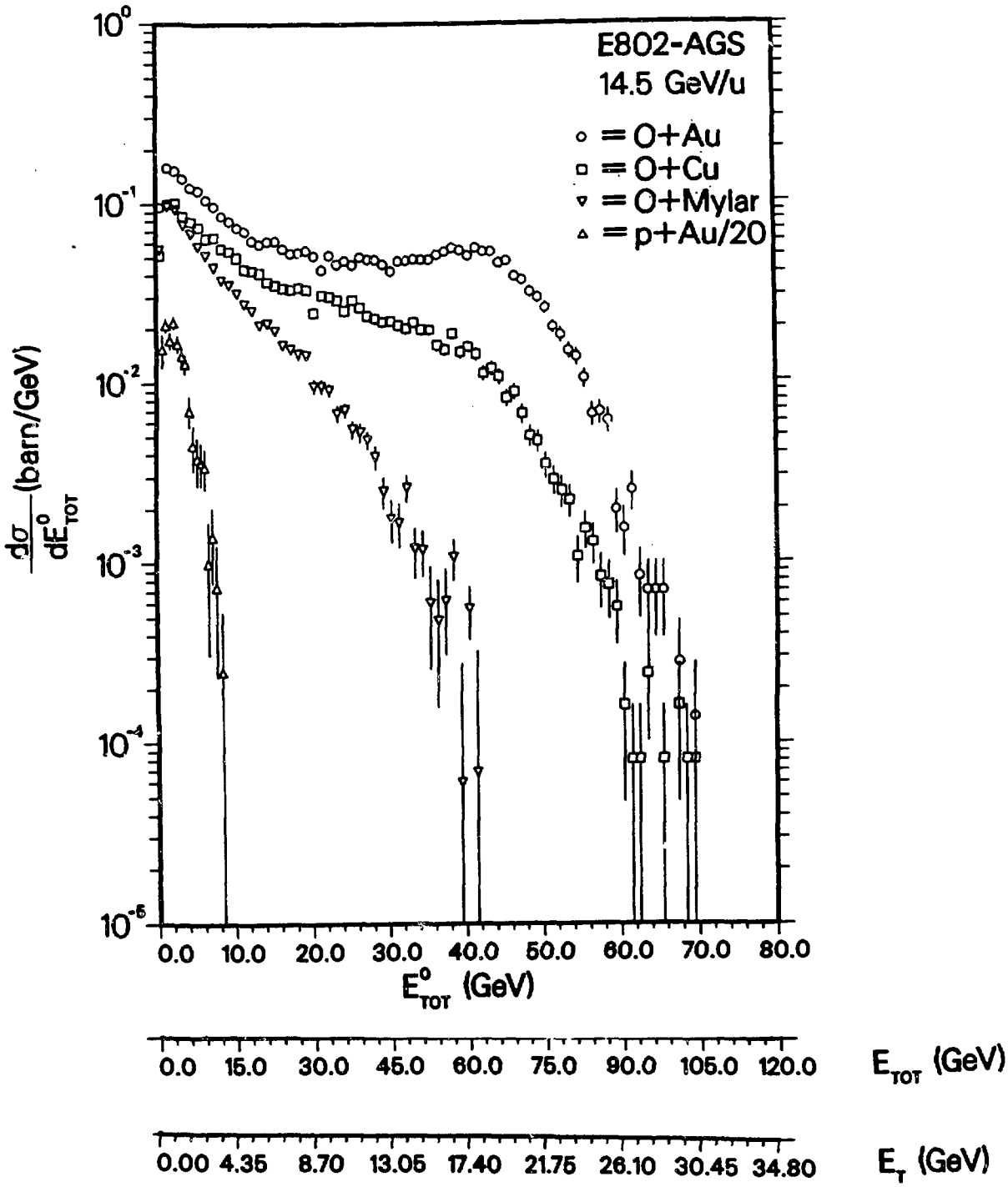
E802-AGS
14.5 GeV/u
○ = O+Au
□ = O+Cu
▽ = O+Mylar
△ = p+Au/20
$\frac{d\sigma}{dE^0_{TOT}}$ (barn/GeV)
10^0
10^{-1}
10^{-2}
10^{-3}
10^{-4}
10^{-5}
0.0 10.0 20.0 30.0 40.0 50.0 60.0 70.0 80.0
E^0_{TOT} (GeV)
0.0 15.0 30.0 45.0 60.0 75.0 90.0 105.0 120.0
E_{TOT} (GeV)
0.00 4.35 8.70 13.05 17.40 21.75 26.10 30.45 34.80
E_T (GeV)

Fig. 2

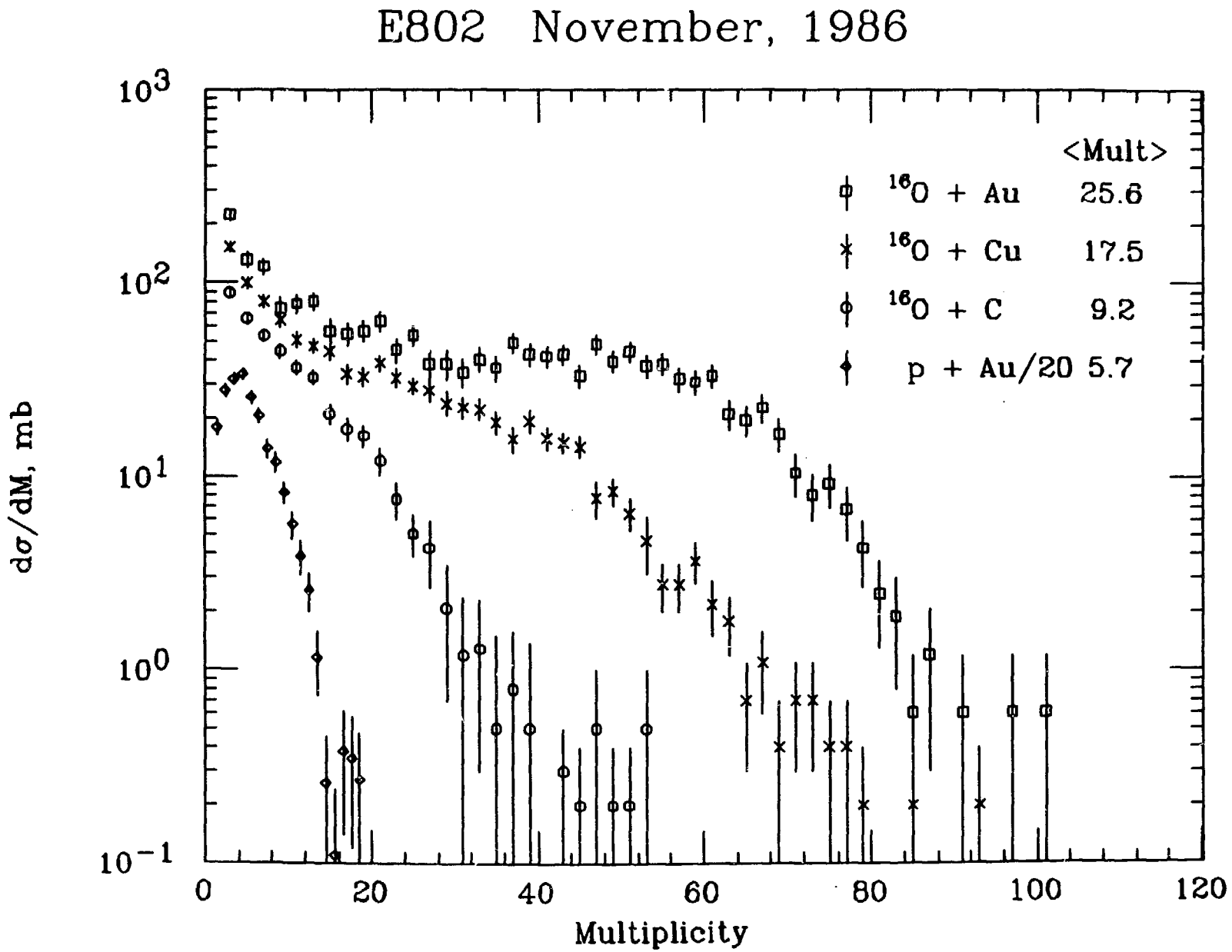
E802 November, 1986
<Mult>
^{16}O + Au 25.6
^{16}O + Cu 17.5
^{16}O + C 9.2
p + Au/20 5.7
dσ/dM, mb
Multiplicity
10^3
10^2
10^1
10^0
10^{-1}
0
20
40
60
80
100
120

Fig. 3

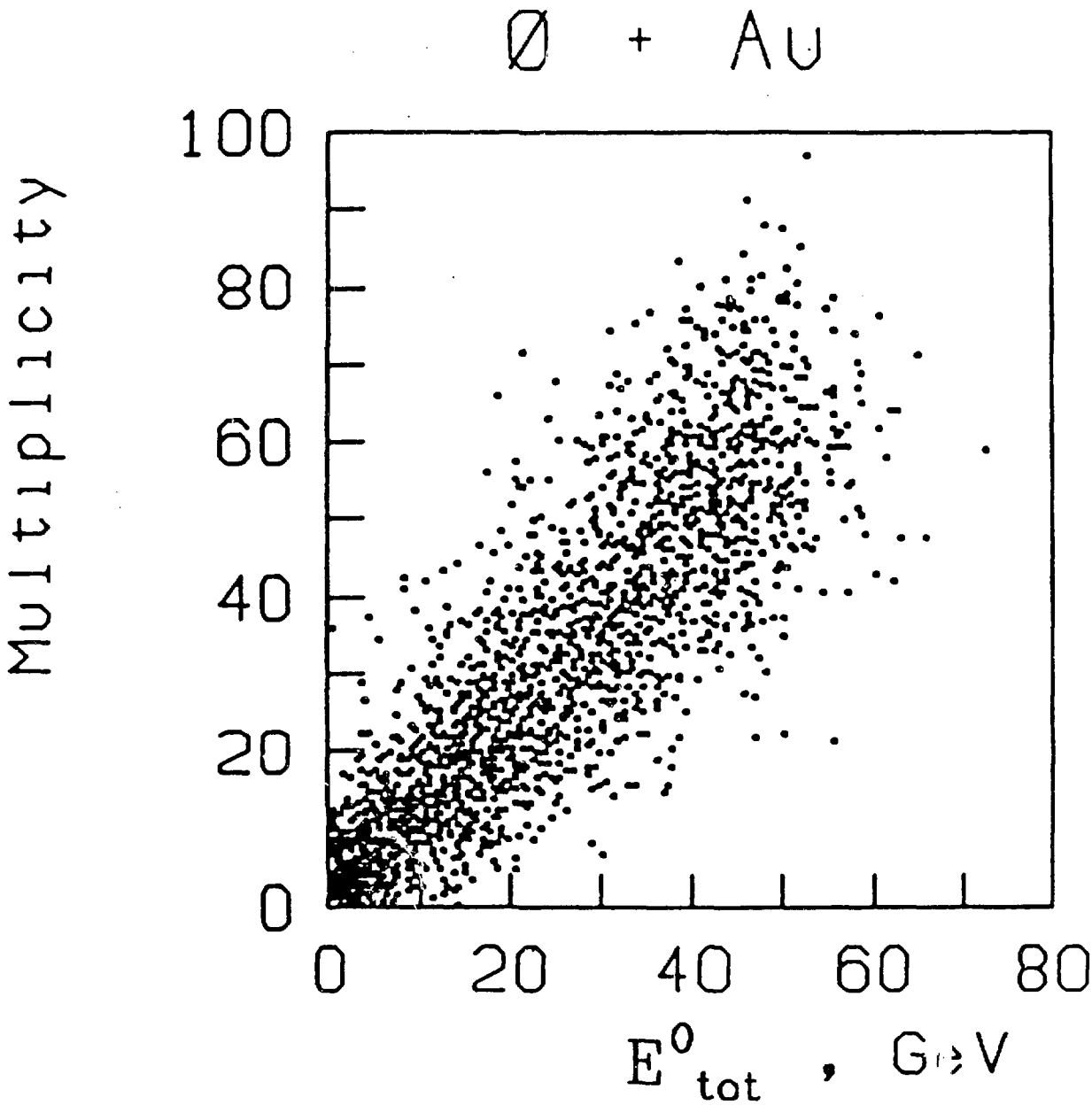

Fig. 4

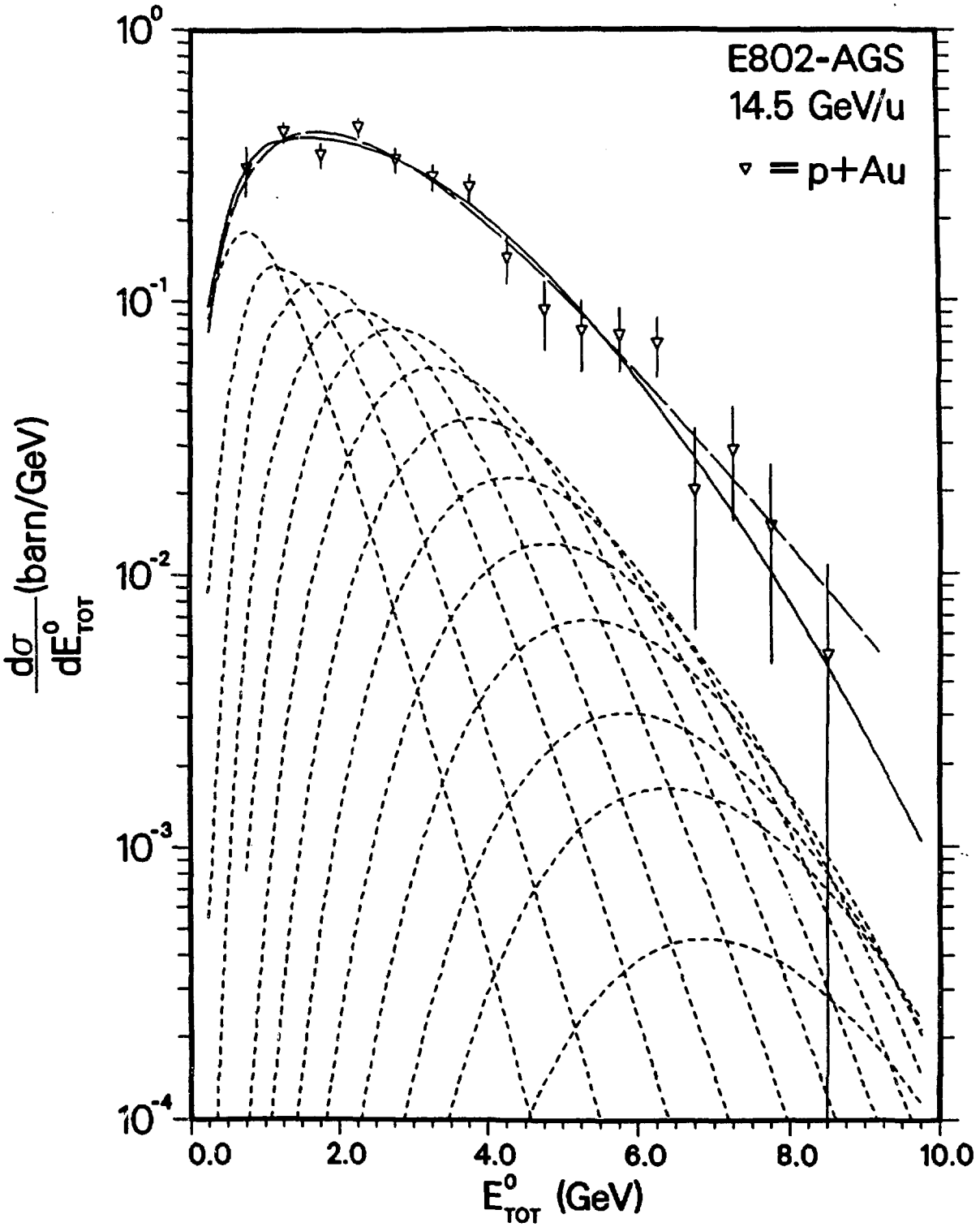
E802-AGS
14.5 GeV/u
▿ = p+Au
10^0
10^{-1}
10^{-2}
10^{-3}
10^{-4}
$\frac{d\sigma}{dE^0_{TOT}}$ (barn/GeV)
0.0
2.0
4.0
6.0
8.0
10.0
E^0_{TOT} (GeV)

Fig. 5

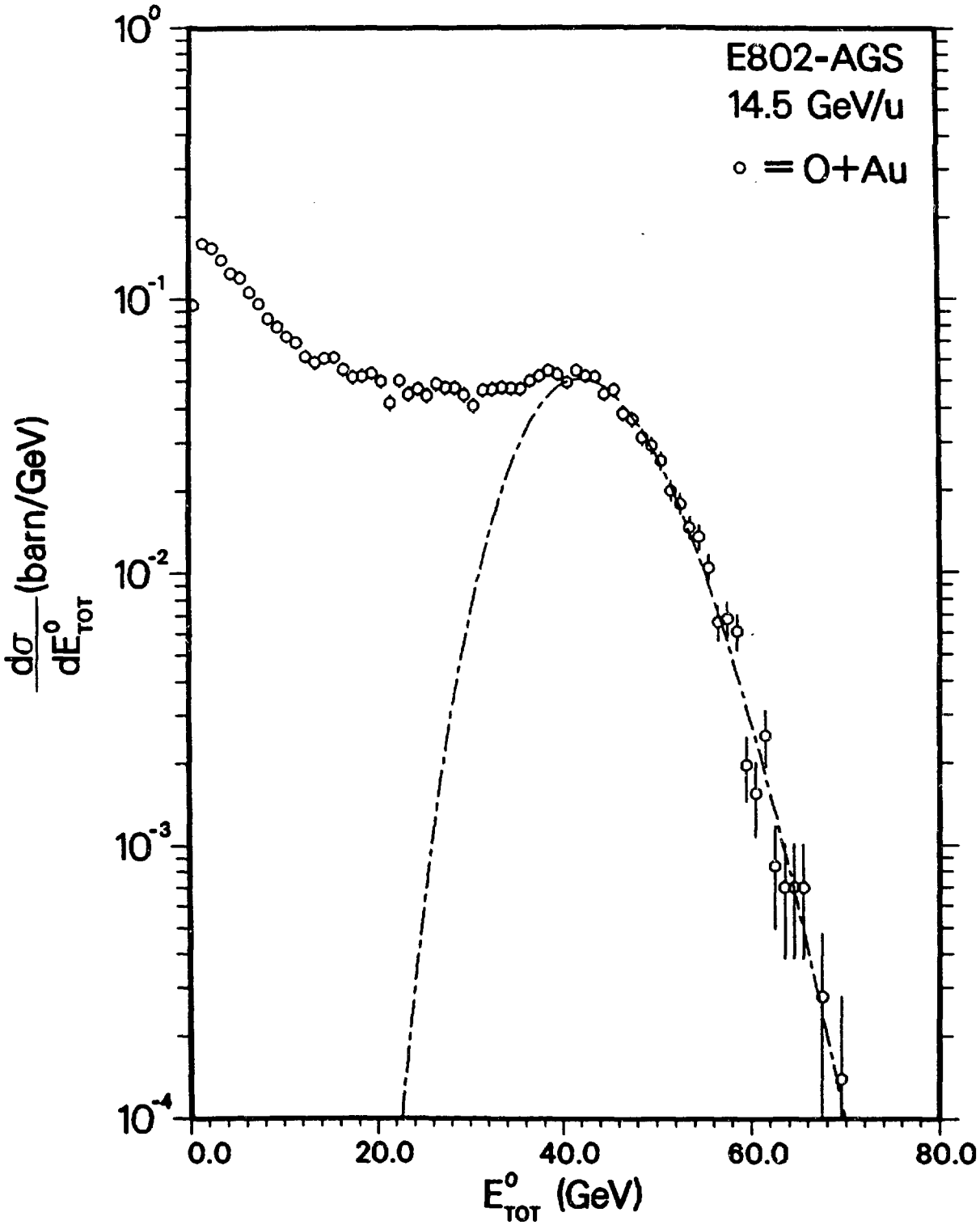
E802-AGS
14.5 GeV/u
○ = O+Au
10^0
10^{-1}
10^{-2}
10^{-3}
10^{-4}
$\frac{d\sigma}{dE^0_{TOT}}$ (barn/GeV)
0.0
20.0
40.0
60.0
80.0
E^0_{TOT} (GeV)

Fig. 6

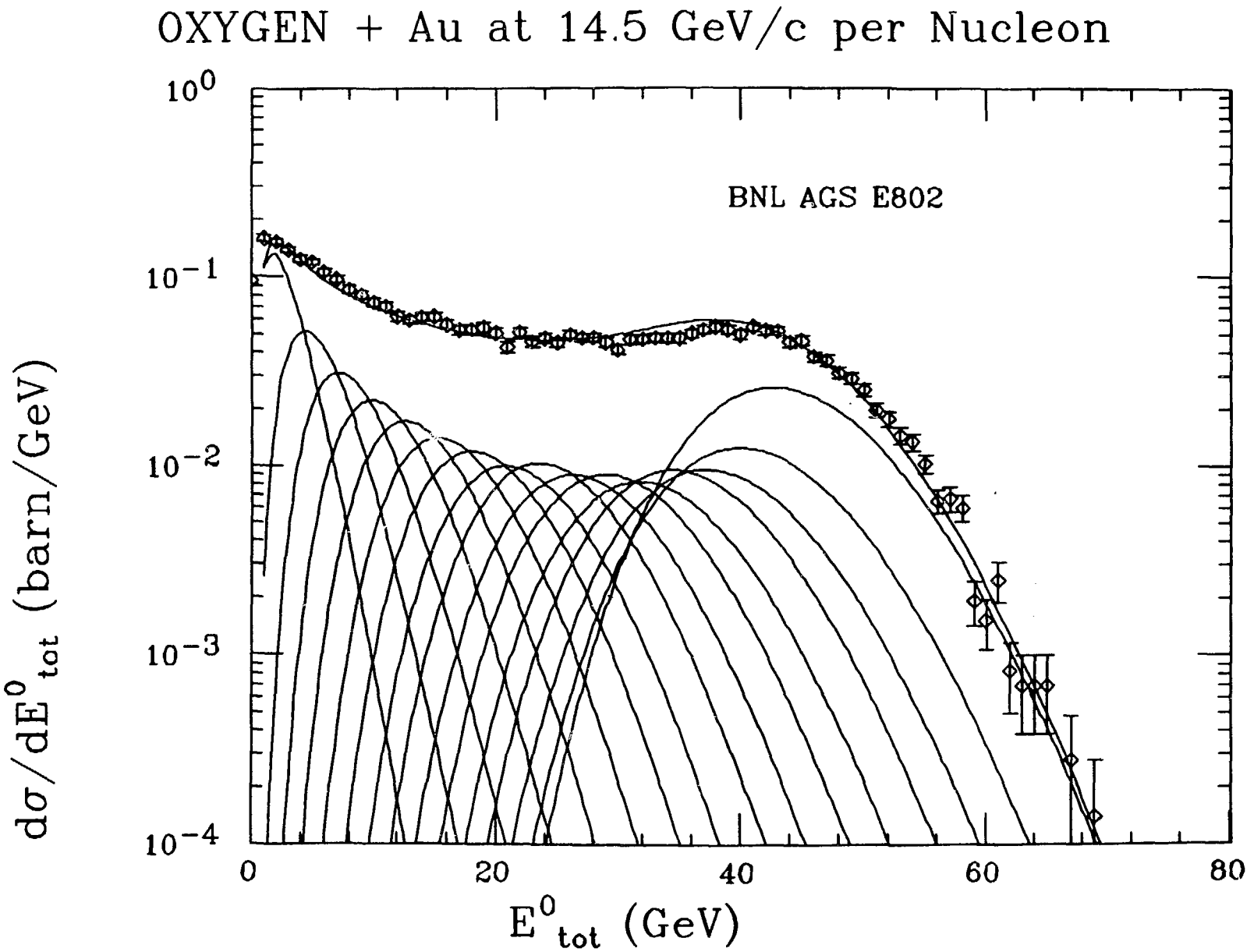
OXYGEN + Au at 14.5 GeV/c per Nucleon
BNL AGS E802
10^0
10^{-1}
10^{-2}
10^{-3}
10^{-4}
$d\sigma/dE^0_{tot}$ (barn/GeV)
0
20
40
60
80
E^0_{tot} (GeV)

Fig. 7a

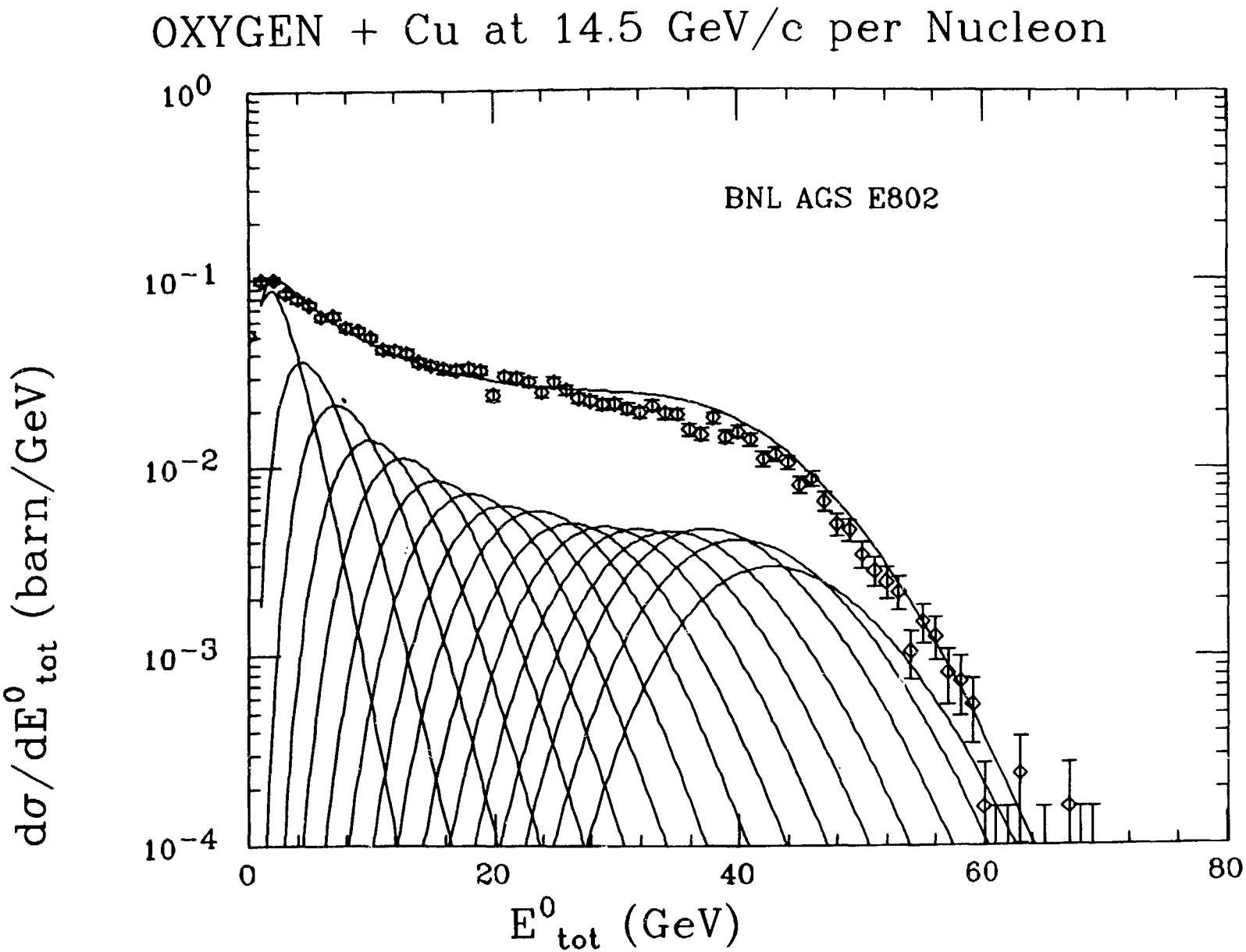
OXYGEN + Cu at 14.5 GeV/c per Nucleon
BNL AGS E802
10^0
10^{-1}
10^{-2}
10^{-3}
10^{-4}
$d\sigma/dE^0_{tot}$ (barn/GeV)
0
20
40
60
80
E^0_{tot} (GeV)

Fig. 7b

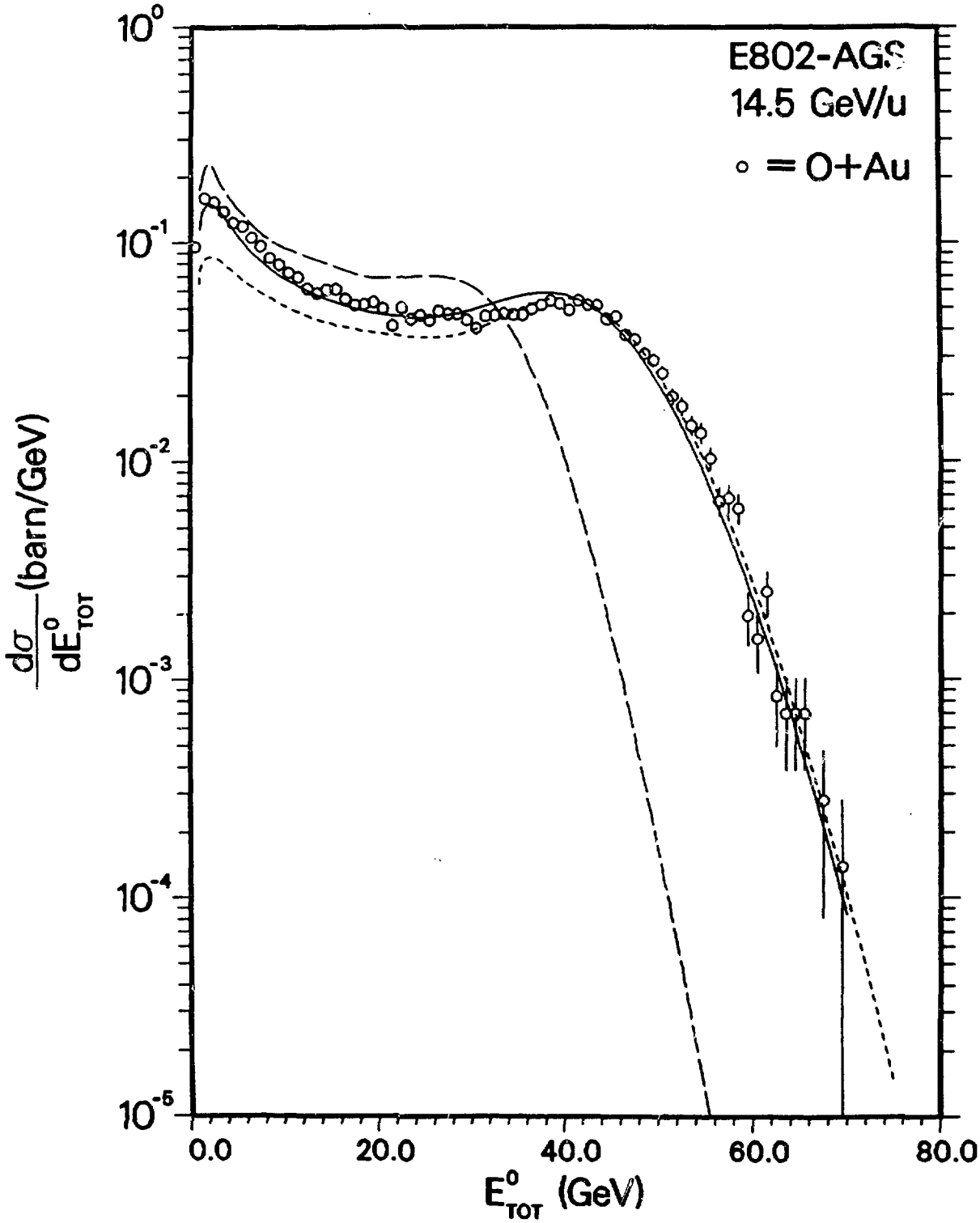
E802-AGS
14.5 GeV/u
○ = O+Au
10^0
10^{-1}
10^{-2}
10^{-3}
10^{-4}
10^{-5}
$\frac{d\sigma}{dE^0_{TOT}}$ (barn/GeV)
0.0
20.0
40.0
60.0
80.0
E^0_{TOT} (GeV)

Fig. 8a

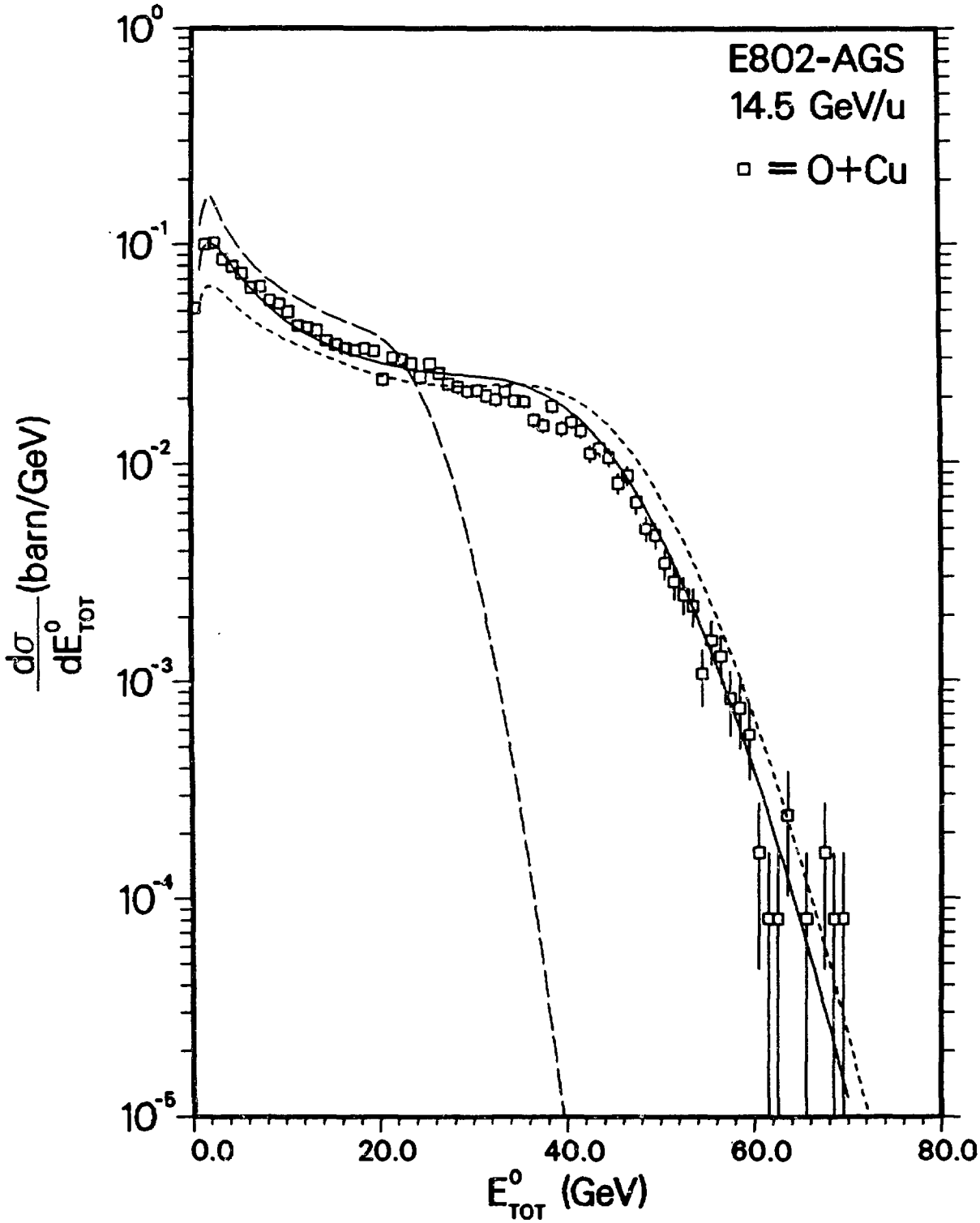
E802-AGS
14.5 GeV/u
▫ = O+Cu
10^0
10^{-1}
10^{-2}
10^{-3}
10^{-4}
10^{-5}
$\frac{d\sigma}{dE^0_{TOT}}$ (barn/GeV)
0.0
20.0
40.0
60.0
80.0
E^0_{TOT} (GeV)

Fig. 8b

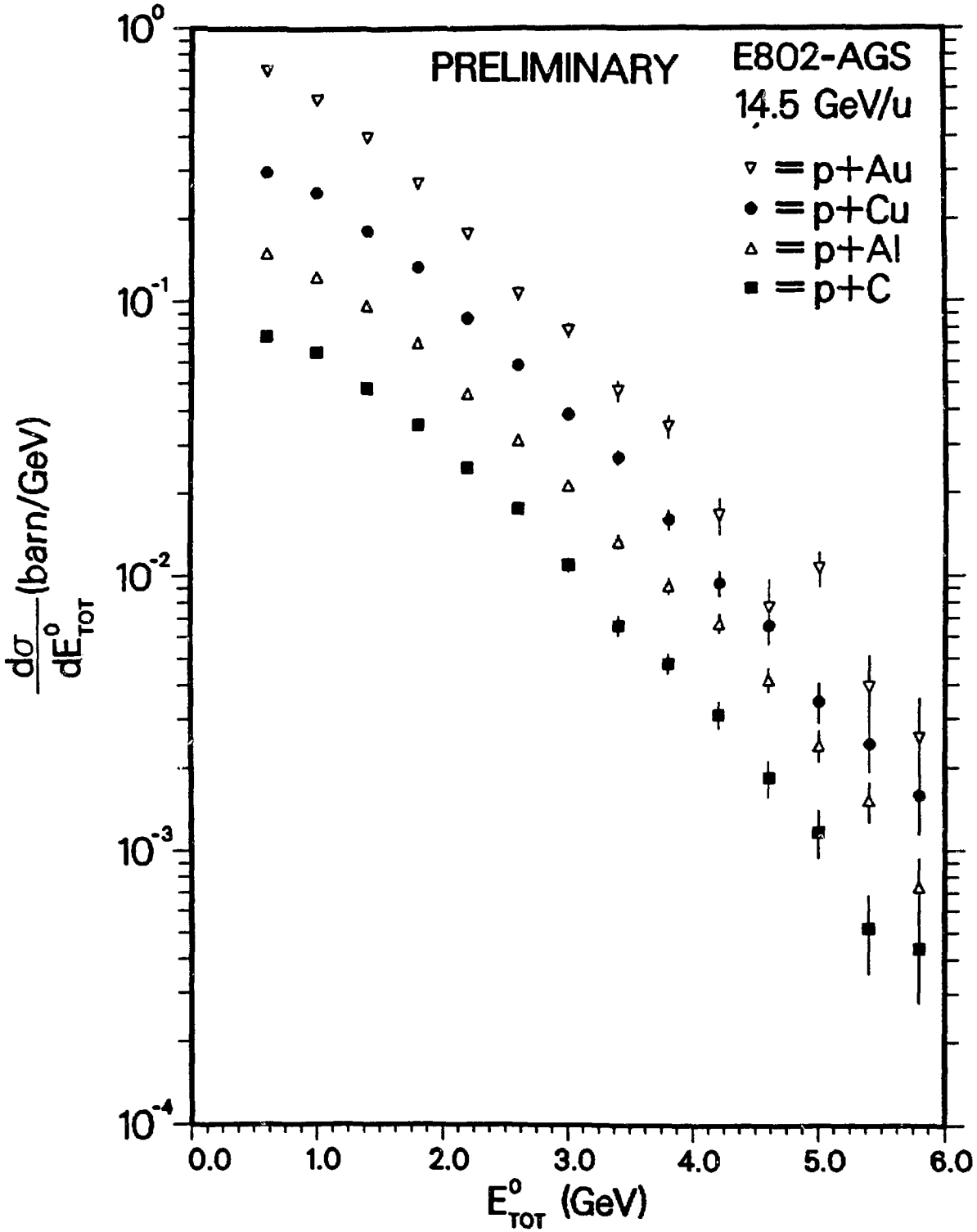
PRELIMINARY
E802-AGS
14.5 GeV/u
▽ = p+Au
● = p+Cu
△ = p+Al
■ = p+C
$\frac{d\sigma}{dE^0_{TOT}}$ (barn/GeV)
E^0_{TOT} (GeV)
10^0
10^{-1}
10^{-2}
10^{-3}
10^{-4}
0.0
1.0
2.0
3.0
4.0
5.0
6.0

Fig. 9

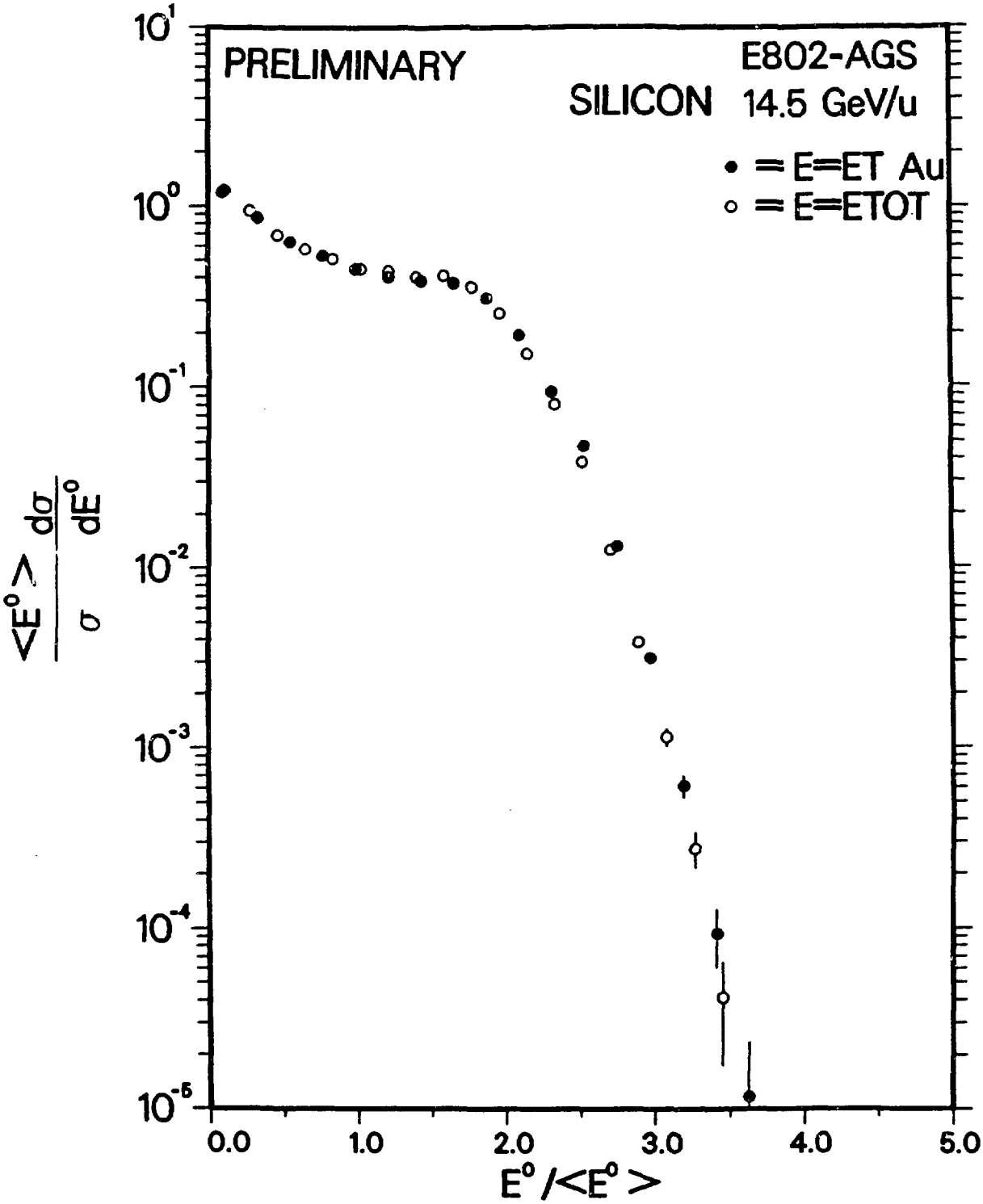
PRELIMINARY
E802-AGS
SILICON 14.5 GeV/u
• = E=ET Au
○ = E=ETOT
$\frac{\langle E^0 \rangle}{\sigma} \frac{d\sigma}{dE^0}$
$E^0/\langle E^0 \rangle$
10^1
10^0
10^{-1}
10^{-2}
10^{-3}
10^{-4}
10^{-5}
0.0
1.0
2.0
3.0
4.0
5.0

Fig. 10a

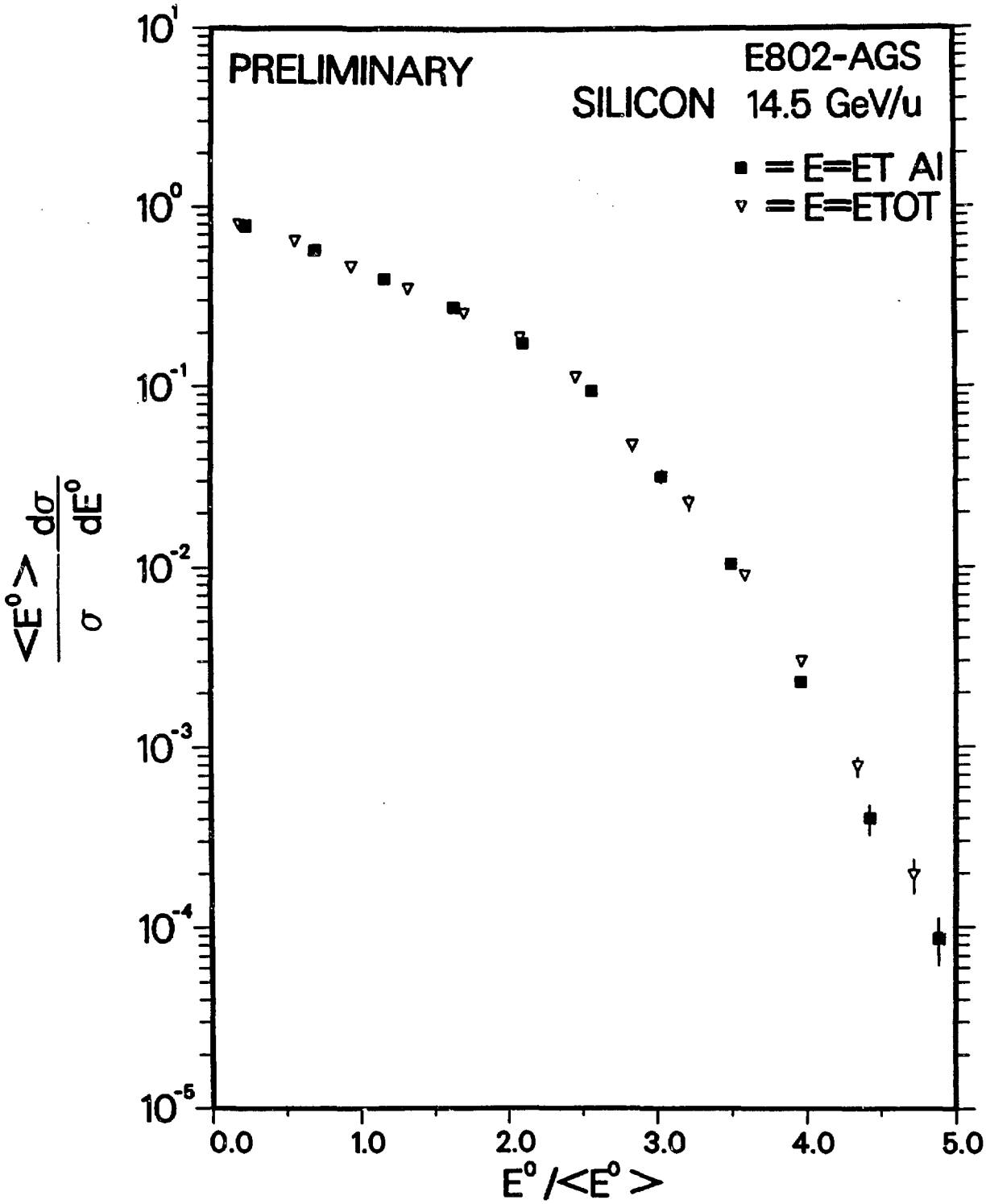
PRELIMINARY
E802-AGS
SILICON 14.5 GeV/u
■ = E=ET Al
▽ = E=ETOT
10^1
10^0
10^{-1}
10^{-2}
10^{-3}
10^{-4}
10^{-5}
$\frac{\langle E^0 \rangle}{\sigma} \frac{d\sigma}{dE^0}$
0.0
1.0
2.0
3.0
4.0
5.0
$E^0/\langle E^0 \rangle$

Fig. 10b

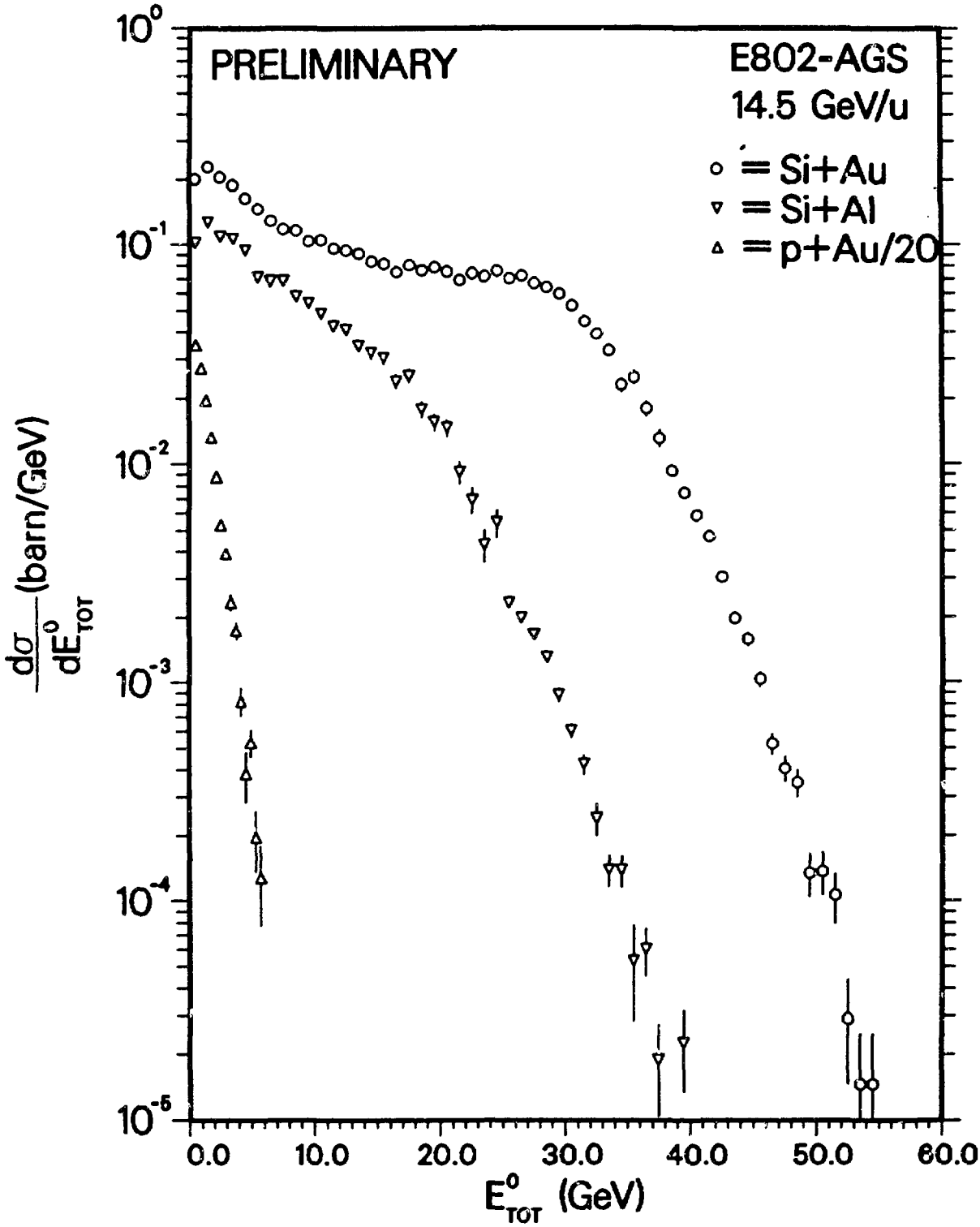
PRELIMINARY
E802-AGS
14.5 GeV/u
= Si+Au
= Si+Al
= p+Au/20
$\frac{d\sigma}{dE^0_{TOT}}$ (barn/GeV)
E^0_{TOT} (GeV)
10^0
10^{-1}
10^{-2}
10^{-3}
10^{-4}
10^{-5}
0.0
10.0
20.0
30.0
40.0
50.0
60.0

Fig. 11

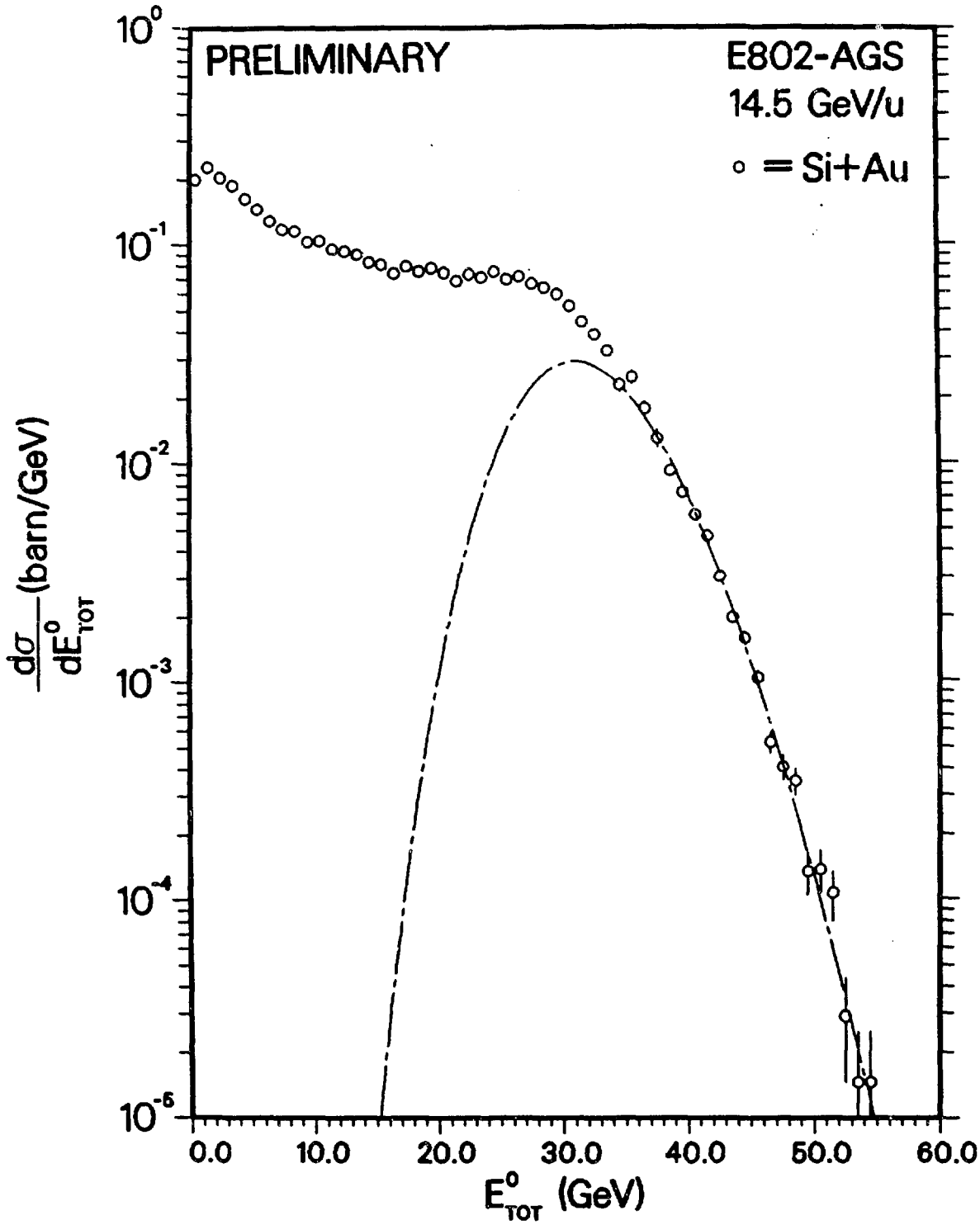
PRELIMINARY
E802-AGS
14.5 GeV/u
o = Si+Au
10^0
10^{-1}
10^{-2}
10^{-3}
10^{-4}
10^{-5}
$\frac{d\sigma}{dE^0_{TOT}}$ (barn/GeV)
0.0
10.0
20.0
30.0
40.0
50.0
60.0
E^0_{TOT} (GeV)

Fig. 12